Studies on nonlinear behaviour of floating components for offshore desalination plants

Ashwani Vishwanath*, Purnima Jalihal and Abhijeet Sajjan

National Institute of Ocean Technology, Ministry of Earth Sciences, Chennai 600 100, India

The article discusses the design considerations for components which exhibit nonlinear phenomenon for an offshore floating platform housing energy and desalination plants. It gives an account of specific cases where such analyses were carried out. National Institute of Ocean Technology, MoES has been working in the area of developing large capacity offshore-based desalination plant. Various platform configurations were studied for housing the plant components. First case study deals with the numerical investigation of an inter-connection system between two floating platforms, semi-submersible and spar platform. Second case describes the methodologies for studying the effects of crucial vortex-induced vibration for estimating the fatigue life of the long-sea-conduit independently and when bundled.

Keywords. Cold water pipe, inter-connection, vortex-induced vibration.

Introduction

THE temperature difference that exists between the warm surface sea water (28°~30°C) and deep sea cold water (7°~15°C) could be effectively utilized to produce potable water and energy from thermal gradient. Because of the availability of the depths greater than 800 m at a distance of 30–40 km from the shore, a plant for energy and water needs to be installed on a floating platform for increased yield. Such platform should be stable and all-weather, so that the process plant, water conduits and an inter-connecting mechanism between conduit and platform can be housed. Based on these requirements, a configuration with a semi-submersible which houses the complete plant and a spar which supports a long, deep cold-water conduit was chosen. The inter-connection system between these platforms needs to allow the independent behaviour of the platforms during operating conditions. One part of the present work focuses on hydrodynamic investigation of coupled behaviour of connected floating structures.

Vijily[1] contributed a method to perform the dynamic analysis of various components of interconnected structural systems such as tanker, yoke, articulated tower, buoy and semi-submersible subjected to regular and random waves in frequency domain. Chakrabarti[2] described an efficient analytical/numerical method that determines the responses of multiple floating structures in waves in the vicinity of each other. Derstine and Brown[3] proposed a compliant connector concept to reduce the large loads that are developed in connecting semi-submersible platforms for a mobile offshore base. Li *et al.*[4] investigated the motion performance of the soft yoke mooring Floating Production Storage and Offloading (FPSO) system in shallow water.

The extensive literature in the area of development of spar and semi-submersible and multibody system is available. It is noted that the complex problem of interconnecting spar and semi-submersible platforms while taking care of motion of both platforms in six degrees of freedom and ensuring fluid transfer between the platforms has not been dealt with in earlier studies. Thus, it is only imperative that an extensive study[5] be carried out to the extent possible in this area.

Various experimental and numerical studies have been reported for Vortex Induced Vibration (VIV) for lower Reynolds numbers and (side length)/diameter (L/D) ratio. Extensive experiments were carried out by Alam[6] on two circular cylinders in a tandem arrangement in a uniform flow at a certain Reynolds number. It was concluded that the fluctuating lift and drag forces acting on a downstream cylinder are very sensitive to the spacing between the cylinders. Each of the fluctuating lift and drag coefficient distributions of the downstream cylinder shows two peaks: one is at $L/D = 0.4$ and the other is at $L/D = 1.4$, where L is side by side distance between cylinders[6]. A numerical study[7] was undertaken for estimating behaviour of VIV for higher Reynolds numbers and L/D ratio suiting our applications. Studies carried out on offshore components to be used for offshore energy and desalination applications are limited. The present paper discusses the analyses of critical areas which are identified for such applications.

Interconnection system between two platforms

Interconnection system description

The inter-connection system is critical in proper functioning of the desalination/process plant. It connects the semi-submersible to a permanently moored spar platform by flexible connectors. The flexible connector helps to

*For correspondence. (e-mail: ashwani@niot.res.in)

relieve the individual platform motion, thereby eliminating the coupled effects. A suitable inter-connection system is conceptualized as shown in Figure 1.

The inter-connection system comprises two sets of rotational joints, horizontal arm frames and yaw reliever arrangement. The rotational joints are fitted at the ends of semi-submersible and spar. This helps in decoupling all the relative rotational and heave motion between the platforms. The fluid transfer between the platforms is through the horizontal arm frames of the inter-connection system. The numerical studies carried out on the inter-connection system involve two stages: (i) hydrodynamic analysis of unconnected platforms and (ii) hydrodynamic analysis of connected platforms. The geometrical characteristics of semi-submersible and spar are given in Tables 1 and 2 respectively.

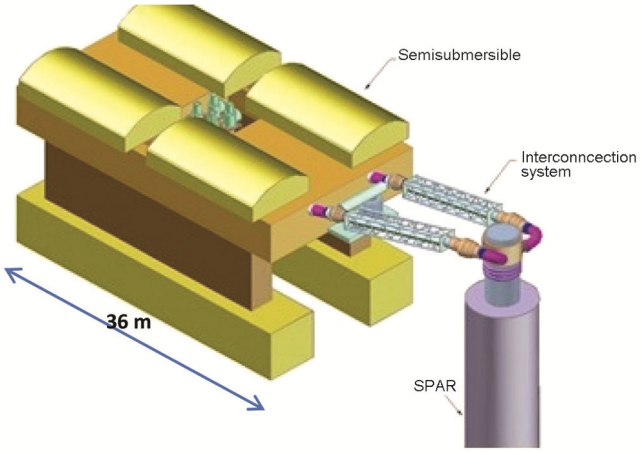

Figure 1. Conceptual model of inter-connection system.

Table 1. Geometrical characteristics of semi-submersible

Deck	
Length, breadth, depth (m)	36, 32, 6
Column	
Length, breadth, depth (m)	9, 5.75, 14
Pontoon	
Length, breadth, depth (m)	36, 10, 10
Operational displacement (mass) (kg)	9343×10^3
Operating draft (m)	19.27
KG (m)	8.79

KG, Centre of gravity from keel.

Table 2. Geometrical characteristics of spar

Diameter (m)	7.5
Length of hull (m)	115
Length of truss (m)	120
Length of bottom tank (m)	7
Draft (m)	226.11
VCG (m)	130.41
VCB (m)	146.88

VCG, Vertical centre of gravity; VCB, Vertical centre of buoyancy.

Hydrodynamic motion analysis of platforms

The complexity of the motion response of offshore floating platform requires advanced simulations tools for the accurate assessment of the sea keeping behaviour. In the current study commercial code 'MOSES' is used which is based on potential/diffraction theory for force estimation.

The potential distribution of the pressure on the panels of the floating platform is given by the linearized Bernoulli eq. (1) for the geometry beneath the water surface[8]

$$p = -\rho\left(gz + \frac{\delta\phi}{\delta t}\right), \tag{1}$$

where ρ is the fluid density, g the acceleration due to gravity, z the depth, ϕ is the velocity potential.

By integrating the pressure over the body, hydrodynamic forces on a portion of the body is obtained. The code calculates the frequency-dependent added mass, damping matrices and in addition all the hydrodynamic properties.

On the basis of the hydrodynamic forces the linear motions in six degrees of freedom are estimated as the RAOs (response amplitude operators) in frequency-domain analysis. This is done using the equations of motions for a freely floating body

$$\sum_{k=1}^{6}[(M_{jk} + A_{jk})\ddot{\eta}_k + B_{jk}\dot{\eta}_k + C_{jk}\eta_k] = F_j(t) \quad (j = 1,\ldots, 6), \tag{2}$$

where M_{jk} is the body mass, A_{jk} the hydrodynamic mass (added mass), B_{jk} the damping coefficient, C_{jk} the restoring coefficient, η the body movement, F_j is the excitation force.

Unconnected case. To study the hydrodynamic interaction effects, spar and semi-submersible were modelled adjacent to each without considering inter-connection system and the RAOs of both structures were estimated using the tool MOSES, which does not calculate the hydrodynamic interaction of two bodies by default. Therefore, the problem was divided into two steps, estimation of the effect of spar on semi-submersible motion and vice versa. Both platforms were modelled at defined position and analysis was carried out for the first body considering the second body as obstacle to consider the hydrodynamic interaction.

Figure 2 shows the RAOs of spar and semi-submersible taking into account the wave interaction effects of one over the other. Peak heave response period for semi-submersible and spar is found to be at 18.5 and 25 sec respectively.

In order to study the effect of distance between the platforms on their respective motions as a result of

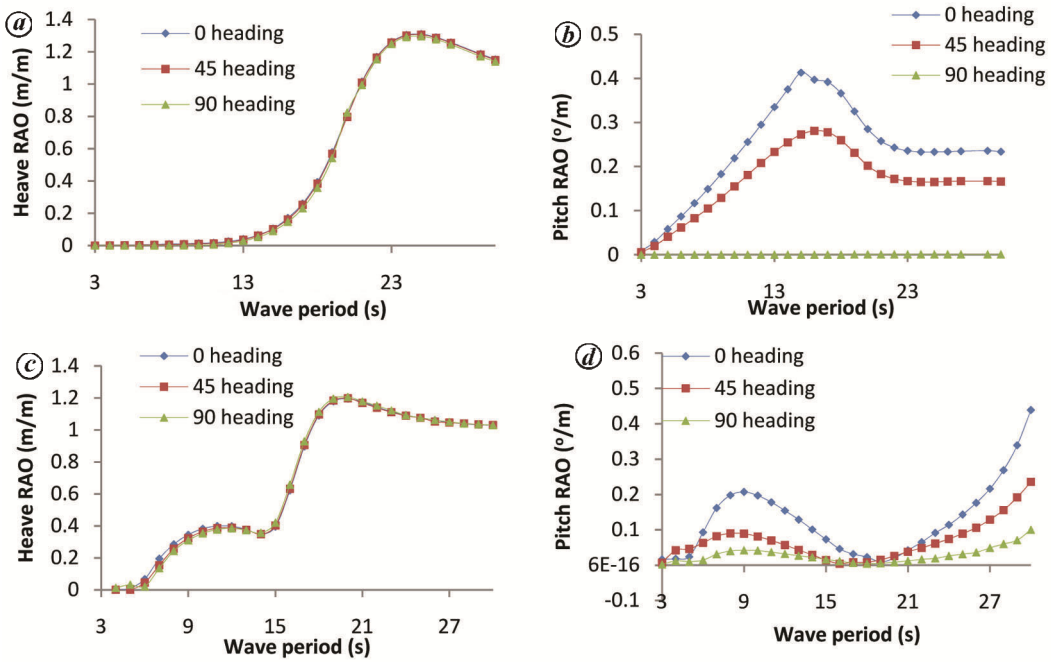

Figure 2. ***a***, Heave RAO of spar; ***b***, Pitch RAO of spar; ***c***, Heave RAO of semi-submersible; ***d***, Pitch RAO of semi-submersible.

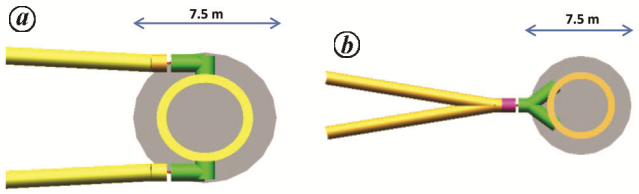

Figure 3. Connector at spar end-earlier (***a***) and modified (***b***).

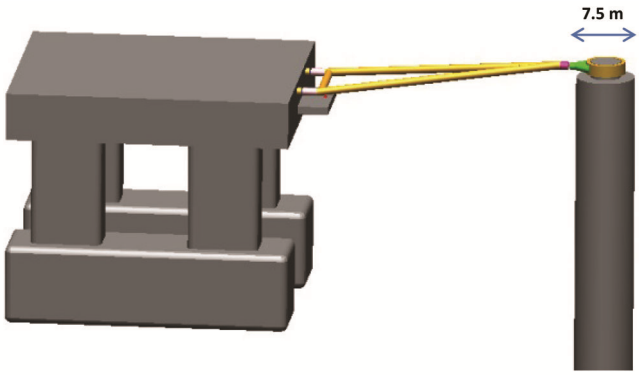

Figure 4. Interconnection model in ADAMS.

hydrodynamic interaction, cases with distance 20 m, 30 m and 40 m were considered for the study. However, no noticeable changes in RAOs were observed in heave and pitch direction for different distances considered. Distance of 20 m between the platforms was taken for further study.

Connected case. In the second stage, the coupled hydrodynamics of the inter-connected system was studied. It is difficult to model the links with flexible joints in MOSES without knowing the range of connector stiffness. Hence, the conceptual model was modelled in 'MSC ADAMS', a rigid body dynamic tool, for the kinematic and dynamic study of the links and joints in the inter-connection system for the given platform motion.

(i) *Modelling inter-connected system using MSC ADAMS.* The inter-connection system along with the two platforms was modelled; it consisted of four spherical joints, four linear springs, a torsional spring and a three-dimensional spring. These springs hereby are referred to as connectors. The platform motions from MOSES with unconnected case were imported to MSC ADAMS as spline functions to mimic prescribed motions for the platform. The first aim was to achieve the dynamic stability of the inter-connection system with the prescribed platform motion. Initially, two parallel horizontal rods were used to connect the platforms and connector stiffness values were assumed. Inter-locking of the link members was observed in the simulation. Later a few modifications were required in the arrangement of the connectors at the spar end to achieve a stable configuration. Figure 3 shows the modification in the arrangement of the connector. Thus with the modification on the conceptual model, the connection was able to give all motions to the platform. The modified configuration is shown in Figure 4.

The flexible connectors are critical elements which decide the forces as well as the flexibility of the interconnection system. The connectors are defined in terms of

Table 3. Axial and rotational stiffness of the connectors

	Axial stiffness along (N/m)			Rotational stiffness about (Nm/°)		
Connector	*X*-axis	*Y*-axis	*Z*-axis	*X*-axis	*Y*-axis	*Z*-axis
C-1, C-2, C-3	5×10^7	8×10^7	8×10^7	10	10	10
C-4	4×10^8	8×10^8	8×10^8	1×10^3	1×10^7	1×10^7

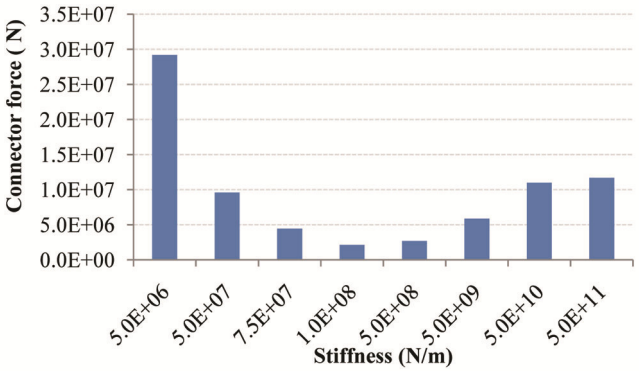

Figure 5. Maximum connector force versus stiffness.

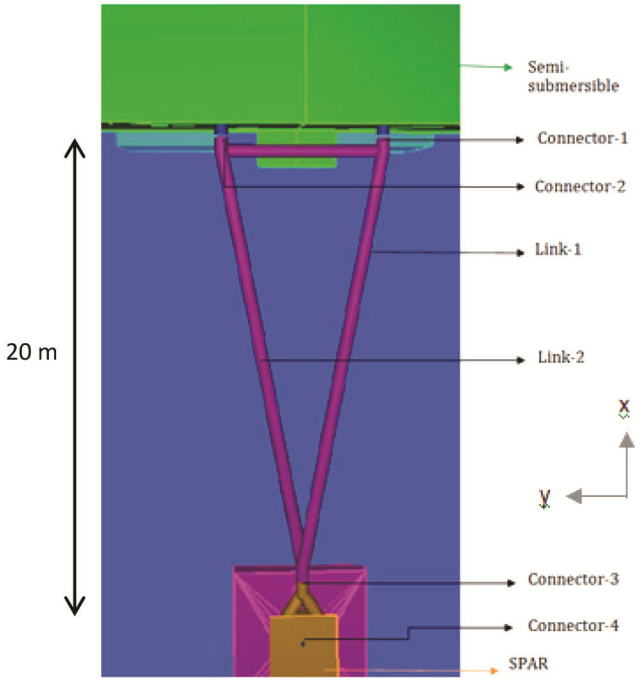

Figure 6. Connectors used in the inter-connection system.

their stiffness. Therefore, deciding the suitable connector stiffness is as important as the connector configuration in the design process. A parametric study was done by varying the connector stiffness and the results are shown in Figure 5.

It was observed that for stiffness values less than 5×10^6 N/m, the system is highly flexible and hence unstable while for stiffness value above 5×10^{11} N/m the spring behaves rigidly and does not have much desired flexible effect on the system. Thus on evaluation of forces on the spherical joint, the suitable connector stiffness was chosen as 1×10^8 N/m.

(ii) *Interconnected platforms in MOSES.* The spar and semi-submersible are now connected using the proposed inter-connection system in MOSES. The inter-connection system consists of tubular members of 1 m diameter and 50 mm wall thickness and four flexible connectors. Spar is moored to the seabed and semi-submersible is connected to spar by the inter-connected system.

The inter-connection system as shown in Figure 6 is connected to the semi-submersible by flexible connectors (connector-1 and connector-2) which are 10 m apart. The inter-connection system is connected to spar by another flexible connector-3. There is a special arrangement (connector-4) for connecting spar to the inter-connection system, which helps to reduce the force transfer from spar to the inter-connection by relieving the spar motion in heave and yaw direction.

These flexible connectors are rotational joints with axial stiffness and hence, the values for rotational stiffness values are taken as negligible. The axial stiffness was taken from the parametric study done in MSC ADAMS. The chosen stiffness values were used to model the inter-connection and the fine-tuning of these values was done to achieve the optimum level of forces and motions. The final connectors' (referred as C-1 to C-4) stiffness values are shown in Table 3.

In order to calculate the forces in connecting members under operating sea conditions, frequency-domain as well as time-domain analysis taking into account all non-linearities of environmental forces, were carried out in MOSES. The frequency-domain analysis of the inter-connected system gives an idea of force in the connector generated due to coupled motions of semi-submersible and spar for each wave period. These forces generated in the connectors (connector load) for unit wave height are explained below.

Since the connector-1 and connector-2 are parallel, the loads for connector-1 and connector-2 are similar. The force along the *x*-axis is significantly higher than the other two directions. Figure 7 *a* shows the connector load for connector-1 and Figure 7 *b* shows the connector load for connector-3. The connector load for connector-1 is

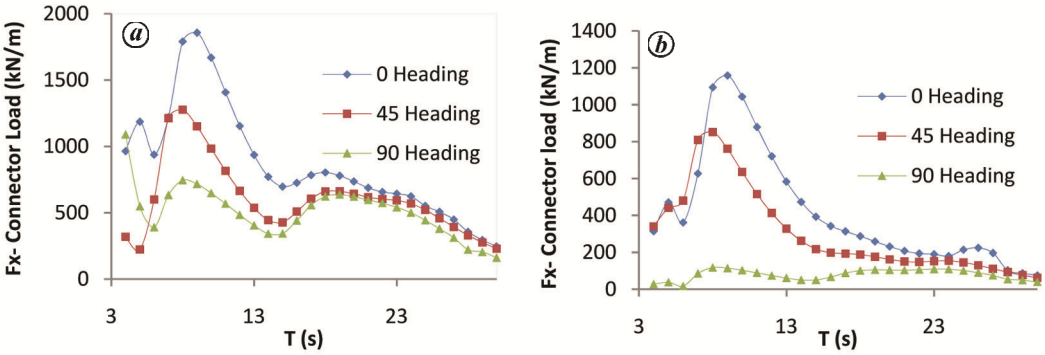

Figure 7. Load RAO of (***a***) connector-1 and (***b***) connector-3.

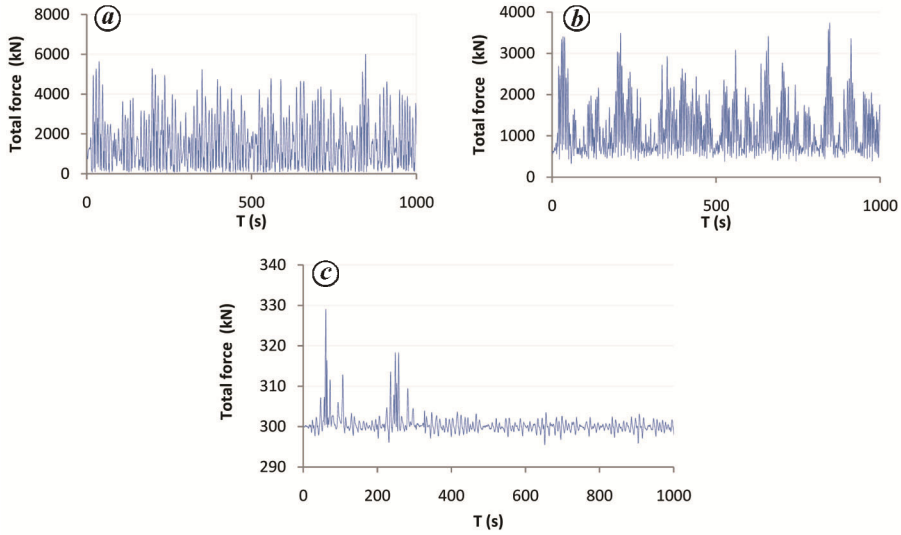

Figure 8. Time series plot for (***a***) connector-1; (***b***) connector-3; (***c***) connector-4.

Table 4. Summary of connector forces

	C-1	C-2	C-3	C-4
Maximum force (*N*)	6001.22	5985.20	3738.5	329.04
Minimum force (*N*)	49.82	43.32	328.85	295.54

maximum for 0° heading in X-direction for a wave period of 9 s of about 1856 kN/m. The connector load for connector-3 is maximum for 0° heading in X-direction for a wave period of 9 s of about 1158 kN/m.

A time-domain simulation taking into account all the non-linear low- and high-frequency external forces for ISSC wave spectrum ($Hs = 5$ m, $T = 10$ s) for 0° wave heading was carried out for estimating the forces in the connectors arising out for a given operating condition. The time history of connector forces is shown in Figure 8. Forces in connector-2 are similar to connector-1 as both are identical joints.

Summary of forces acting on the connection members as obtained from the simulation is shown in Table 4. The estimated forces are then used for carrying out structural analysis of the inter-connection components.

VIV analysis of deep sea conduits

Large diameter HDPE pipes

The studies discussed here establish a methodology for design of long-deep-sea-cold-water pipes for fatigue caused due to VIV. Spar platform discussed earlier is used to support the cold-water pipe while providing mooring for the semi-submersible housing the plant equipments. The deep sea cold-water and surface warm-water are conveyed to the plant equipment installed on the deck by multiple large diameter high density polyethylene (HDPE) pipes connected at the top deck of the platform. These long and slender conduits are susceptible to nonlinear forces such as VIV due to ocean currents and vessel motions which could lead to fatigue damage. These conduits are inherently buoyant which

advantageously reduce the payloads on the deck and aid in towing during installation. The conduit is subjected to maximum stress at the top end and is subjected to fluctuating loads in the splash zone. The pressure differential across the wall is insignificant as the pipes are open at the bottom end. The stress–strain relationship is entirely nonlinear and is strongly influenced by the duration of loading, stress levels, temperature, etc. The permissible design stress to be allowed is thus dependent on the design life of the pipes as the material exhibits creep.

VIV of water intake pipe

VIV is caused due to the periodic shedding of vortices due to flow separation over a bluff body. The frequency of shedding depends on diameter of the body and the velocity of flow. High amplitudes of vibrations occur when the frequency of vortex shedding coincides with the natural frequency of the structure. VIV can bean important reason for fatigue damage of riser pipes used in thermal desalination.

For a 3D-structure the vortex shedding occurs in cells in the span wise direction and with different vortex shedding frequencies. When the pipe is subjected to shear flow along its length, the multi-modal vibrations are setup. VIV is influenced by the mass ratio (m^*) defined as the ratio of the mass of the structure to the mass of the displaced fluid. The HDPE pipes have mass ratio of less than 1. The synchronization of the vortex shedding frequency to Strouhal and natural frequencies depends on the mass ratio. The procedure for estimating the effects of VIV given in DNV-OS-F201 (ref. 9) has been outlined in this section.

Methodology. Methodology adopted to evaluate the amplitude of vortex induced vibration, stress range and the associated fatigue damage is described below.

Vortex shedding frequency (fs) is calculated as per clause 103 of DNV-OS-F201 (ref. 9). The frequency (fs) obtained is considered as 'cross flow vortex shedding frequency' and $2 \times fs$ to be considered as inline vortex shedding frequency.

Amplitude (A) is calculated using equation E2, clause 104 of DNV-OS-F201.

$$\frac{A}{\gamma D} = \sqrt{0.32/(0.06 + 2\pi * S_t^{\,2} * K_s)}, \tag{4}$$

where S_t is the Strouhal number, K_s the stability parameter, γ is the mode participation factor.

Mode participation factor (γ) is calculated as per clause 9.5.3 of DNV-RP-C205 (ref. 10). The values of mode shape (Y_x) and maximum shape value (Y_{max}) is taken directly from FE analysis for each mode shape.

$$\gamma = Y_{\max} \left(\frac{\int_0^L Y^4(x)\mathrm{d}x}{\int_0^L Y^4(x)\mathrm{d}x} \right)^{1/2}. \tag{5}$$

Stability parameter is determined using equation from section 9.1.8 of DNV-RP-C205.

$$K_s = \frac{2 * m_e \delta}{\rho D^2}, \tag{6}$$

where m_e is the effective mass per unit length of conduit and D is the diameter of the conduit and $\delta = 2\pi\xi$.

Strouhal number is determined corresponding to relevant Reynolds number as per figure 9.1 of DNV-RP-C205.

The VIV stress range (S) is calculated as per clause 105 of DNV-OS-F201, stress concentration factor (SCF) is considered as 1, the curvature of mode shape (k) is calculated as per equation E4, clause 105 of DNV-OS-F201.

$$S = A \text{ SCF } k\,(D - t). \tag{7}$$

where A is the amplitude of vibration, SCF the stress concentration factor and k is the curvature of mode shape.

$$k = \left(\frac{\partial^2 \phi}{\partial s^2} \cdot \left(1 + \left(\frac{\partial \phi}{\partial s} \right)^2 \right)^{-3/2} \right),$$

where s is the location of the concerned node and ϕ represents displacement of the node.

After determining the stress range, fatigue damage is calculated as per clause 106 of DNV-OS-F201.

$$D_f = \left(\frac{F_n \cdot T_L}{a} \right) \cdot S^m, \tag{8}$$

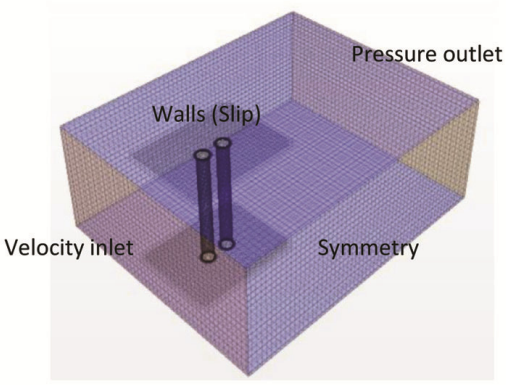

Figure 9. Domain and mesh.

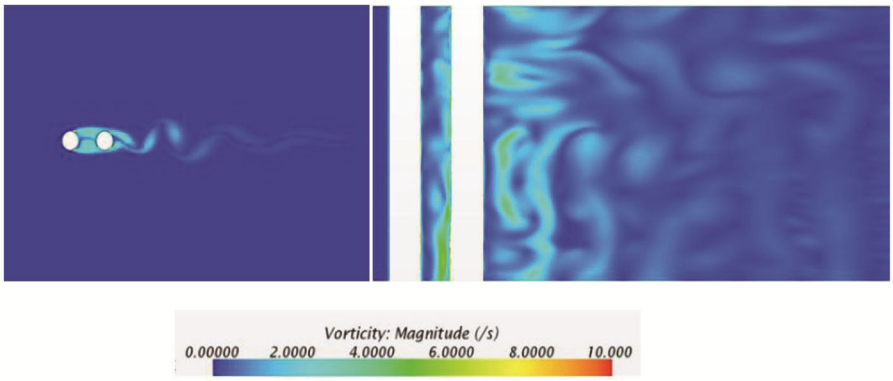

Figure 10. Vortex shedding along the cross-section and span.

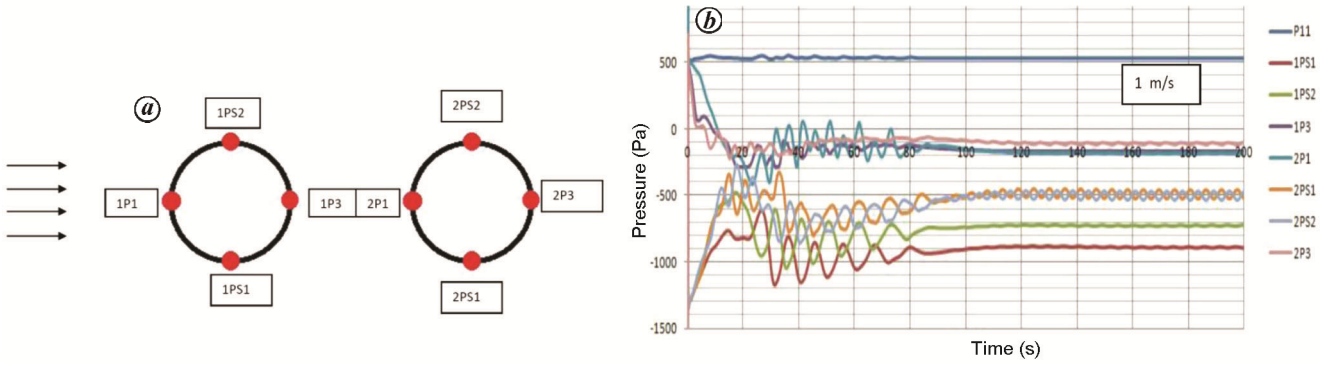

Figure 11. Pressure monitors around (***a***) the pipes and (***b***) the upstream and downstream pipe.

where F_n is the natural frequency of the relevant mode shape, T_L the design life of the conduit, a the characteristic fatigue strength constant of the material and m is the fatigue exponent of the material.

The methodology outlined here will help in determining the extent of VIV influence in design of independent deep sea conduits.

VIV of pipe bundle

In the current project, the multiple seawater intake and discharge pipes are bundled together which requires alternate methods like computational fluid dynamics (CFD) techniques to estimate velocity, pressure distributions around the individual pipes. The local normal velocities thus estimated are used to calculate vortex shedding frequencies and thus helps in selection of resonant modes for VIV calculations using the above mentioned methodology.

When the pipes are bundled together, vortex shedding can either happen entirely on the pipe bundle or locally on the individual pipes. In cases of local vortex shedding, the VIV of a pipe is influenced by the pipes in their near vicinity known as 'wake interference'. The wake interference may cause the destabilizing lift and drag forces causing higher vibration amplitudes in crossflow and inline directions. Hence it is crucial to study the VIV of multiple pipes in a bundle. The VIV of single pipe and pipes arranged in tandem configuration studied using CFD is discussed in this section (for spacing/diameter = 2; $Re = 0.8 \times 10^6$–3.2×10^6).

The domain and mesh generated is shown in Figure9. The lift, drag co-efficients are estimated for upstream and downstream pipes. Figure 10 shows the vortex shedding patterns over the cross-section and along the span length. The pressures predicted all around the upstream and downstream pipe with reference to Figure 11 *a* are given in Figure 11 *b*.

The pressure difference is predicted to be higher on the upstream pipe in both inline and crossflow direction which results in higher drag and lift forces on the pipe. It was predicted that the pressures across the downstream pipe in inline direction were reduced due to the wake created by the upstream cylinder and reattachment of the vortices leading to decrease in its drag co-efficient. Figure 12 *a* compares the drag co-efficient for upstream, downstream and for independent single pipe. Figure 12 *b* shows the lift co-efficients for pipes at Re of 1.6×10^6. It was found that the vortex shedding frequency of downstream pipe is altered due to wake interactions and decrease in the lift co-efficient was observed. Cd and Cl values for independent single pipe are predicted to be higher as compared to bundled pipes for the spacing to diameter ratio used.

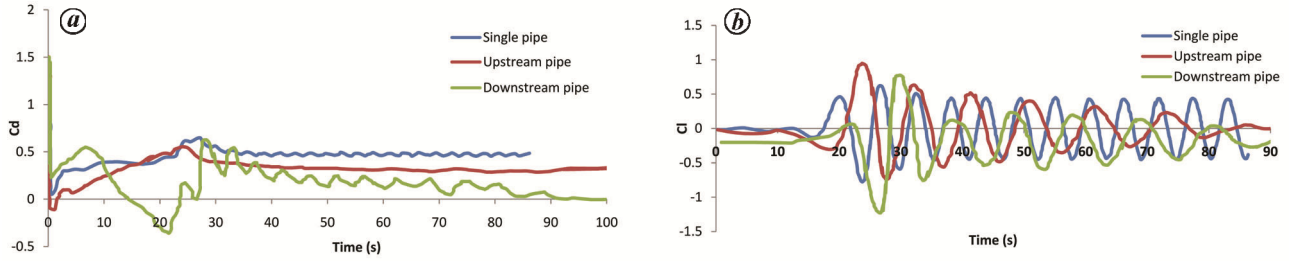

Figure 12. ***a***, Drag co-efficient for Re 1.6×10^6 (flow velocity = 1 m/s); ***b***, Lift co-efficients for Re 1.6×10^6.

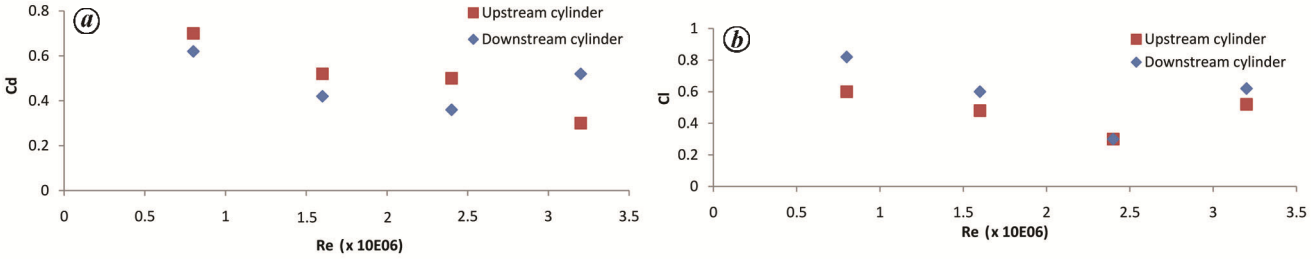

Figure 13. Variation of (***a***) Cd and (***b***) Cl with Reynold's number.

Figure 13 *a* and *b* shows the variation of Cd and Cl respectively with Reynold's number for both upstream and downstream pipes. A sharp drop in the lift co-efficient was observed at Reynold's number of 2.4×10^6 and then it increases which could be due to the turbulent boundary layer separation.

The upstream pipe will have larger displacement in both directions in comparison to the downstream cylinder owing to the differences in the lift and drag forces generated and could lead to the collision of the adjacent pipes. This condition could be detrimental for the pipe bundle and hence plays crucial role in choosing the spacing between the pipes.

Conclusions and future work

The present paper discusses the critical areas of offshore components which require special attention in the overall design for a floating desalination plant in 1000 m of water depth. A numerical investigation of a semi-submersible and a spar inter-connected by a flexible inter-connection system was carried out to study the wave-induced motions and connector loads. The stiffness in axial and rotational direction at the joints was arrived at, and forces were estimated to design the desired inter-connection system to allow independent behaviour of the platforms while being integrally connected during operating conditions.

The deep sea conduit design methodology is outlined in line with global practices. The effect of VIV on individual and bundle of pipes is clearly outlined for estimating the design life of conduits. The flow behaviour around the single pipe and pipe bundle was studied using CFD. In case of pipe bundle, drag and lift forces were found to be higher on the upstream pipe in comparison to the downstream pipe for the spacing to diameter ratios used. These differences in the respective forces could be detrimental to the pipe bundle and shall form the governing criteria in determining the spacing of the pipes in a bundle. Experiments for physical insight into the behaviour of these components will be carried out.

1. Vijily, B., Dynamic analysis of interconnected offshore structural systems subjected to random waves. Ph D thesis, Indian Institute of Technology Madras, 1997.
2. Chakrabarti, S. K., Response due to moored multiple structure interaction. *Mar. Struct.*, 2001, **14**, 223–258.
3. Derstine, M. S. and Brown, R. T., A compliant connector concept for the mobile offshore base. *Mar. Struct.*, 2000, **13**, 399–419.
4. Li, X., Yang, J. and Xiao, L., Research on motion response of soft yoke mooring FPSO system. In Proceedings of Sixteenth International Offshore and Polar Engineering Conference, San Francisco, California, USA, 2006.
5. Sreekumar, P., Numerical investigations of a flexible interconnection system between a semi-submersible and a spar platform, M Tech thesis, IIT Madras, 2014.
6. Alam, M. M., Sakamoto, H. and Zhou, Y., Determination of flow configurations and fluid forces acting on two staggered circular cylinders of equal diameter in cross-flow. *J. Fluids Struct.*, 2005, **21**, 363–394.
7. Jaya Chandran, S. R., A CFD study on vortex induced vibration of circular conduits, M Tech thesis, IIT Madras, 2017.
8. Chakrabarti, S. K., *Hydrodynamics of Offshore Structures*, WIT Press, 1987.
9. DNV-OS-F201, Dynamic risers-rules and standards, October 2010.
10. DNV-RP-C205, Environmental conditions and environmental loads, October 2010.

ACKNOWLEDGEMENT. We gratefully acknowledge the Ministry of Earth Sciences for their support for this work.

doi: 10.18520/cs/v118/i11/1694-1701